Proceedings of ERAD 2006

Cell-oriented forecasts of Czech weather radar data

Petr Novák[1], Hana Kyznarová[2,1]

[1] Czech Hydrometeorological Institute, Radar department.

[2] Charles University, Faculty of Mathematics and Physics.

1 Introduction

The Czech Weather Radar Network (CZRAD) consists of two Doppler C-band weather radars, which cover the entire area of the Czech Republic and vicinity using a volume scan coverage with a 10-min update rate up to 256 km range (Novák and Kráčmar, 2002). The most frequently used radar product is maximum reflectivity composite field. Volume reflectivity information can be obtained from CAPPI fields between 1 and 14 km. All products have 1km horizontal and 0.5km vertical resolution that enables good interpretation of radar echoes.

Several severe weather events (floods, flash floods, hail, tornadoes) that occurred on the territory of the Czech Republic within the last decade highlighted the importance of weather radar measurements and their utilization in nowcasting systems. In the beginning of 2003 two prediction methods were implemented into operational processing of CZRAD (Novák, 2004). Both methods are used for prediction of entire radar image domain. The COTREC method extrapolates CZRAD composite images by the wind field determined by comparison of two consecutive maximum reflectivity fields using the mean absolute difference as similarity criterion. The second method uses for extrapolation wind field derived from the geopotential at 700hPa calculated from numerical weather prediction model.

These methods work well but they have some limitations mainly for severe convective storms nowcasting. These limitations resulted into development of CELLTRACK, cell-oriented algorithm for radar echo prediction, in the Czech Hydrometeorological Institute (CHMI).

2 CELLTRACK - algorithm description

2.1 Identification of reflectivity cores

Several methods like SCIT (Johnson at al., 1998) or TRACE3D (Handwerker, 2002) were developed to identify and track reflectivity cores in radar images. Identification of cores with high reflectivity, as an approximation of convective cells, is different in individual methods and is dependent on their purpose.

To identify reflectivity cores CELLTRACK uses single reflectivity threshold of 44 dBZ. This threshold was final choice after testing of several other values (36, 40, 44, 48 dBZ). Main reason for choosing 44 dBZ threshold was a compromise between identification of weaker cells (lower values of threshold) and better distinguishing of individual reflectivity peaks in clusters of convective cells (higher values).

An identification algorithm derived from TRACE3D method was also tested. As input it used reflectivity cores obtained by identification utilizing single threshold of 44 dBZ. Then it found local maximum in each reflectivity core and removed all values lower than the local maximum reflectivity value - 10 dBZ.

TRACE3D based algorithm is more suitable for identification of individual cells especially in clusters of convective cells. Different quantities of peak reflectivity within the reflectivity core can be tracked. However, this algorithm is not suitable for monitoring of storm volume development and other quantities, as reflectivity threshold of the reflectivity core varies during its lifetime. This problem is removed when a reflectivity core is defined by single reflectivity threshold. Justification for this method lies in operational utilization, where it is important to predict movement of areas of high reflectivity instead of only reflectivity peaks. Furthermore, according to preliminary results, CELLTRACK tracking skill is slightly better for single threshold algorithm reflectivity cores rather than for TRACE3D identification algorithm reflectivity cores.

2.2 Reflectivity cores assignment

Assignment algorithm uses two consecutive files of 2D objects identified by one of the above mentioned algorithms

Correspondence to: Petr Novák.

petr_novak@chmi.cz

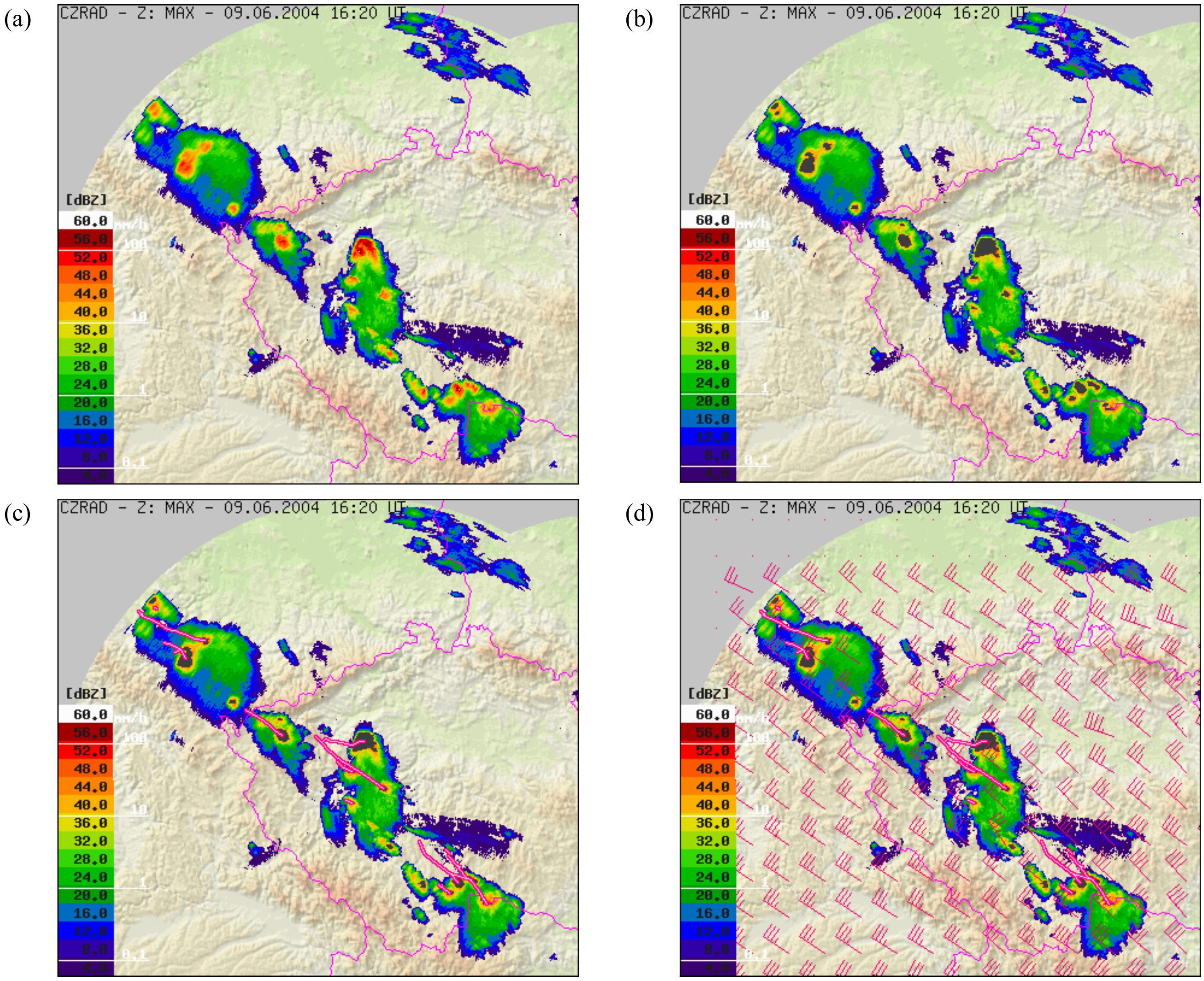

Fig. 1. June 9, 2004 16:20 UTC. (a) Reflectivity scan at 16:20 UTC; (b) the same as (a), but overlayed by appropriate reflectivity cores identified by single threshold algorithm; (c) paths of reflectivity cores drawn back in time, but no more than to 14:50 UTC; (d) same as (c) but overlaid by wind field obtained from COTREC at 15:20 UTC..

as input data. Like other cell tracking algorithms this algorithm uses first guess of reflectivity core movement. For this purpose we use output from COTREC, which is presently operationally calculated in CHMI. For performance of CELLTRACK this approach is better than use of movement vectors derived from previously assigned reflectivity cores. The most important reason for this fact is that CELLTRACK can provide completely misguiding movement vector in case of wrong assignment. On the contrary COTREC movement vector may not be that accurate, but there is lesser probability of computing markedly poor movement vector, that results from design of the algorithm. After calculating first guess, distances and shape similarity between all shifted reflectivity cores and all real reflectivity cores in subsequent image are calculated.

To calculate shape similarity the shifted reflectivity core from the first image is overlaid by reflectivity core from the subsequent image. Values of maxima and minima in x and y direction determine a rectangle drawn to this area. Shape similarity is calculated as $(YY + NN)/(YY + NN + YN + NY)$, where YY is equal to the number of pixels occupied by both reflectivity cores, NN is equal to the number of unoccupied pixels in the rectangle and finally YN and NY are pixels occupied by only one reflectivity core. Another possible quantity could be the root mean square error or the mean absolute error, but the calculation would be more difficult without any significant improvement. Any reflectivity core which is closer than certain radius is marked as possible *child* core (hereafter 'child' only). Moreover each child is tested the same way to have another *parent* core (hereafter 'parent' only). Threshold value grows with increasing mean wind speed and its values lie between 7 and 13 km.

In the next step, algorithm tries to assign reflectivity cores. Clusters (i.e. at least one child and one parent) are processed at first. By tracking a cluster of closely spaced objects on a time series of images there is an increased requirement for shape similarity. Determining a child using criterion of smallest distance is insufficient because of frequent splitting and merging of reflectivity cores as artifact of their identification. The algorithm therefore looks for most similar reflectivity cores in the first step. Their similarity must be higher then minimum of 0.85. If their distance is smaller than threshold mentioned above, they are coupled together (assigned as parent and child) and because of high similarity they are eliminated from further processing of given cluster.

After all pairs of similar cells are found, the program seeks for closest cells. Such a pair must fulfill a criterion of minimal similarity 0.80. If this criterion is not fulfilled the algorithm tries to find other child or parent (i.e. splitting if child is too small or merging if parent is too small). In case of splitting a new child is found if its center lies in the body of first guess reflectivity core or at most two kilometers apart from its edge. The same procedure is applied for merging.

After all clusters are processed the algorithm looks for unassigned cores. A reflectivity core can be unassigned if it has no child or parent or because of splitting and merging. If a sufficiently large core is splitted or it forms from more smaller cores, it may not be assigned to the same cluster, as their centers are too far from each other. Thus, as the last step, assignment algorithm attempts to correct this flaw by searching for splitting and merging of unassigned reflectivity cores. However criteria are somewhat more strict, since centers of smaller reflectivity cores should be inside the body of the larger one. This requirement prevents assigning small distant reflectivity cores, because large reflectivity cores fulfill this criterion very well. The algorithm has no upper limit of number of children and parents.

2.3 Extrapolation of reflectivity core movement

Position of reflectivity core is determined by position of its center; however simple extrapolation of the center of reflectivity core doesn't give satisfactory forecast. Main reason for this poor performance is splitting and merging of reflectivity cores – in most cases artificial product of reflectivity core identification.

Therefore CELLTRACK tries to find best fitting overlay of parents and children in each cluster of reflectivity cores assigned as parents and children. To calculate this overlay true reflectivity values in first image (parents) Z_p are subtracted from true reflectivity values in second image (children) Z_{ch} and quantity sum is calculated using formula

$$sum = n\left(\sum_{n\in X}\left|Z_p(n) - Z_{ch}(n)\right|\right) \qquad (1)$$

where X is area covered by united parents and children areas and n is number of pixels covered in X area. CELLTRACK tries to find smallest value of the sum.

If a reflectivity core has no parent, mean motion vector of reflectivity cores with at least one parent is used. If there is no reflectivity core with at least one parent, no prediction is made. This typically occurs with onset of first detectable reflectivity core. Prediction is made up to 90 minutes with 10 minute time step.

3 Evaluation of performance

Evaluation of CELLTRACK performance was carried out in two ways. Firstly, CELLTRACK performance was evaluated during assignment of reflectivity cores in consecutive radar images. Secondly, skill of CELLTRACK forecasts was compared with COTREC and persistence forecast.

During evaluation of reflectivity cores assignment, assignments obtained from the CELLTRACK algorithm were compared with those obtained from manual inspection (i.e. manual reflectivity cores assignment). In case of difference between them, assignment from manual inspection was labeled as correct, and CELLTRACK assignment was labeled as false. This means if CELLTRACK algorithm assigned *child* and *parent* incorrectly, both number of misses and wrong assignments were increased. Table 1 plots values of hits, misses and wrong assignments of reflectivity cores identified by single threshold algorithm of 44 dBZ. Table 2 presents the same quantities for identification algorithm based on TRACE3D. Four convective situations with various amounts of reflectivity cores and various wind speeds were chosen.

Table 1. Hits, misses, wrong assignments and CSI for four different convective situations and their totals for identification by single threshold algorithm.

Date	hits	misses	wrong assign.	CSI
2001-05-31	369	32	22	0.87
2003-06-08	198	3	5	0.96
2004-06-09	270	19	17	0.88
2004-08-07	181	22	15	0.83
total	1018	76	59	0.88

Table 2. Hits, misses, wrong assignments and CSI for four different convective situations and their totals for identification algorithm based on TRACE3D identification.

Date	Hits	misses	wrong assign.	CSI
2001-05-31	386	34	22	0.85
2003-06-08	181	7	15	0.89
2004-06-09	290	35	29	0.82
2004-08-07	178	26	23	0.78
total	1035	102	99	0.84

The best CSI values were obtained for 2003-06-08 - a situation with few (not more than 10) reflectivity cores in each image. The worst CSI values were obtained for 2004-08-07, which is situation with higher number (between 25 and 30) of reflectivity cores in each image and very slow wind. Remaining two situations have also relatively high number (about 20) of reflectivity cores in each image; however the wind speed is considerably higher.

Forecasting skill and comparison with COTREC were evaluated only for reflectivity cores identification by simple threshold algorithm. We focused on convective situation with presence of deviating storms. Such a situation, 9th June 2004, is presented in fig. 1. In fig. 1(a) there is maximum reflectivy field of convective cells at 16:20 UTC, in fig. 1(b) maximum reflectivity field is overlaid by appropriate reflectivity cores calculated by single threshold algorithm of 44 dBZ. Paths of reflectivity cores identified on the 16:20 UTC image are drawn back in time but no more than to 14:50 UTC in fig. 1(c). In the center of the fig. 1(c) path of storm deviating from the mean wind direction to the left can be seen. Fig. 1(d) is fig. 1(c) overlaid by corresponding wind field calculated by COTREC method. As can be seen, COTREC smoothes wind field in the area of deviating storm.

Fig. 2 displays CSI of forecasts up to 90 minutes for COTREC, CELLTRACK and persistence method on 9th June 2004. It can be seen that CELLTRACK gives slightly better results than COTREC. Performance of persistence forecast is worse than both CELLTRACK and COTREC.

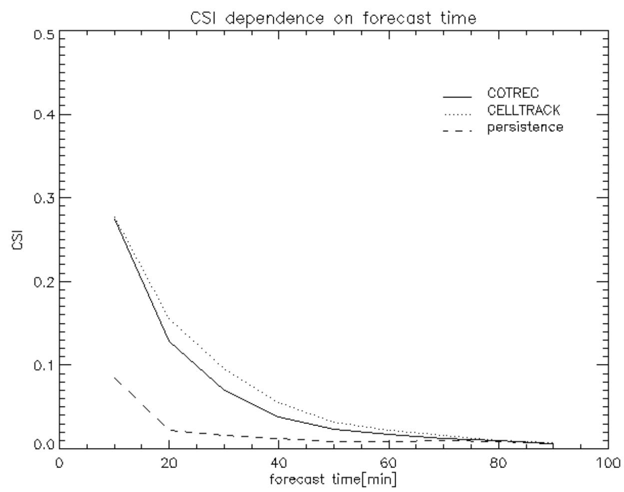

Fig. 2. June 9, 2004. Daily averaged CSI dependence on forecast time for reflectivity value threshold 44 dBZ. Full line represents COTREC, dotted line represents CELLTRACK and dashed line persistence forecast.

4 Conclusions and outlook

CELLTRACK algorithm was developed and tested in the CHMI. Preliminary results indicate that in convective situations this algorithm is able to give forecast comparable with that of COTREC and better than persistence forecast. Therefore it seems to be a suitable complement for COTREC in convective situations. CELLTRACK could be improvement of COTREC especially during occurrence of strong deviating storms (typically supercells). Further improvement of the CELLTRACK forecast can be achieved by means of incorporating lifecycle characteristics derived from volume radar data and other remote sensing methods.

Acknowledgements: This research is supported by the Czech Republic Ministry of Education through grant 1P05ME748 and by the grant GA CR 205/04/0114.

References

Johnson, J.T. et al., 1998: The Storm Cell Identification and Tracking Algorithm: An Enhanced WSR-88D Algorithm, *Weather and Forecasting* **13**, 263 – 276

Handwerker, J., 2002: Cell tracking with TRACE3D – a new algorithm, *Atmospheric Research* **61**, 15 – 34

Novak P., Kracmar J., ,2002,: New data processing in the Czech weather radar network, In: ERAD 2002 proceedings, *ERAD publication series*, **1**, 328-330

Novak P. (2004): Czech weather radar data utilization for precipitation nowcasting, In: ERAD 2004 proceedings, *ERAD publication series*, **2**, 459-463.